



# Surface integrity enhancement of ZL109 aluminum-silicon piston alloy employing the forward and reverse finish cutting method

Hu Sun<sup>1,2</sup> · Anhai Li<sup>1,2</sup>  · Yonghui Zhou<sup>1,2</sup> · Xuhao Song<sup>1,2</sup> · Chaoyi Xue<sup>1,2</sup>

Received: 1 July 2019 / Accepted: 28 January 2020 / Published online: 18 February 2020  
© Springer-Verlag London Ltd., part of Springer Nature 2020

## Abstract

The machined surface integrity has significance on fatigue life. The step-by-step feed cutting is put forward and adopted to machine ZL109 aluminum-silicon piston alloy. In addition, the forward and reverse finish cutting is also proposed to improve the machined quality and fatigue life. The result indicates that the step-by-step feed cutting can effectively avoid scratching and decrease surface roughness, bring about the compressive residual stress, and improve machined quality. Moreover, there is smaller elastic-plastic recovery and thermal expansion on the machined surface, when the step-by-step feed cutting is adopted, so that the machining dimension accuracy can be ensured perfectly. The forward and reverse finish cutting can effectively decrease the surface roughness and the tensile residual stress due to the thermal stress. So the larger the cutting thickness is, the smaller surface residual stress is, when the cutting depth is 0.15–0.30 mm in the forward and reverse finish cutting. It can improve the machined quality of ZL109 aluminum-silicon piston alloy and the fatigue life when the reasonable cutting parameter is adopted. Those results have an important practical significance.

**Keywords** Surface integrity enhancement · ZL109 aluminum-silicon piston alloy · Multi-step machining · Step-by-step feed cutting · Forward and reverse finish cutting

## 1 Introduction

The piston bears huge mechanical stress and thermal stress in the high temperature and pressure working condition. There is huge inertia force due to the high-speed reciprocating motion. The high temperature brings about piston skirt expansion and the cylinder liner's lateral pressure results in severe wear. The piston is prone to fatigue due to the thermal-mechanical coupling and the wide force range in engine. The eutectic ZL109 aluminum-silicon piston alloy (AlSi12CuMgNi) has a good mechanical property, casting, and cutting property. Moreover, there is high-hardness silicon particles (1000 HV) evenly distributed in the bulk. Therefore, ZL109 aluminum-silicon

piston alloy also has a high wear resistance. In addition, its density is smaller than iron, which can decrease inertia force in the piston reciprocating motion, so much that is widely adapted to piston material [1–4]. However, the result shows that high machined quality in production of ZL109 aluminum-silicon alloy is not easy to obtain. There are shortcomings of ZL109 aluminum-silicon piston alloy in cutting: (1) Tool wear severe. High-hardness silicon particles can effectively improve wear resistance. But it is prone to react with carbon elements in tool materials and bring about silicon carbide in cutting, which aggravates tool wear and decreases the machined quality. (2) The chip scratches the machined surface. Cutting ZL109 aluminum-silicon piston alloy will bring about the strip chip being prone to scratch, decreasing the machined surface. In addition, built-up edge produced during cutting aluminum alloy can also decrease the machined quality. (3) The machined dimensional accuracy is not easy to control. The constant extrusion process is cutting. A lot of cutting heat will be produced in cutting process. There are elastic-plastic recovery and thermal expansion on the machined surface which affect the dimension accuracy. (4) Processing bring about tensile residual stress. Surface residual stress is due to that the mechanical stress leads to the plastic deformation and

✉ Anhai Li  
anhaili@sdu.edu.cn

<sup>1</sup> Key Laboratory of High Efficiency and Clean Mechanical Manufacture of MOE, School of Mechanical Engineering, Shandong University, Jinan 250061, People's Republic of China

<sup>2</sup> National Demonstration Center for Experimental Mechanical Engineering Education, Shandong University, Jinan 250061, People's Republic of China

the thermal stress results in the plastic strain [5]. The cutting heat will bring about the surface expansion in processing. And the surface cooling and shrinkage will result in tensile residual stress eventually. The results indicate that surface residual stress is mainly affected by plastic strain due to thermal stress, when cutting edge is sharp completely [6, 7]. Moreover, tensile residual stress decreases the fatigue life significantly.

The processing surface integrity has an important effect on the fatigue life. El-Helieby and Rowe [8] studied the effect of the reverse bending carbon steel bringing about surface residual stress on the fatigue performance. The result indicates that the carbon steel's fatigue life is closely related to the surface residual stress. The larger the surface residual stress is, the smaller the fatigue life is. The compressive residual stress can effectively improve the fatigue life. Jeelani and Musial [9] studied the effect of machining 2024-T351 aluminum alloy surface integrity on fatigue life. The results show that the machined surface integrity significantly affects the 2024-T351 aluminum alloy's fatigue performance. The higher the cutting speed is, the greater the fatigue life is. This is mainly because the compressive residual stress decreases with the cutting speed increasing. In addition, the machined quality is bad in low-speed cutting, so that the fatigue life is low. James, et al. [10] studied the surface residual stress versus fatigue performance. The result indicates that the surface residual stress has a significant effect on the fatigue life. Tensile residual stress can decrease the workpiece fatigue life. Compressive residual stress can improve the fatigue life significantly. Zou et al. [11] studied the effect of the abrasive water jet shot peening the carburized GDL-1 steel surface integrity on fatigue performance. The result shows that the fatigue life can improve by 19% after shot peening; meanwhile, the location of the fatigue source is far away from the machined surface. It is mainly due to the abrasive water jet shot peening bringing about the grain refinement on the surface layer and the compressive residual stress.

The greater the machined surface roughness is, the more serious the surface stress concentration is, eventually resulting in the fatigue life decreasing. Arola and Williams [12] studied the machined AISI 4130 CR steel surface integrity versus fatigue stress concentration. The results show that the high-cycle fatigue life decreases when the surface roughness increases from 2 to 6  $\mu\text{m}$ . Novovic et al. [13] summarized the effect of surface morphology and integrity on fatigue performance. The results indicate that if the machined surface roughness exceeds 0.1  $\mu\text{m}$ , the surface roughness can have an important effect on the fatigue life. But the influence can be neglected if the machined surface roughness is less than 0.1  $\mu\text{m}$ , when considering residual stress is neglected. Ardi et al. [14] discussed the effect of the processed nickel-based superalloy surface finish on the fatigue life. The results show that turning brings about the plow groove being generally the source of the fatigue crack initiation, which decreases the

fatigue life significantly. Andrews and Sehitoglu [15] established a computer model about rough surface versus fatigue crack initiation and propagation. The results show that the fatigue life depends greatly on the surface roughness. But the material's inherent defects will significantly decrease the effect of the surface roughness on the fatigue life. Suraratchai et al. [16] studied the effect of the machined aluminum alloy surface roughness on the fatigue performance. The result indicates that cutting results in the grooves bringing about the stress concentration, which can decrease the fatigue life.

It indicates that the moderate hardening can effectively prevent surface crack initiation and improve the fatigue life. However, the excessive hardening will lead to the spalling and crack initiation [17], which not only does prevent cracks but also accelerates fatigue. Li et al. [18] studied the effect of machined TC4 titanium alloy surface integrity on fatigue performance. It indicates that machined hardening, grain refinement, and compressive residual stress can effectively prevent the fatigue crack initiation and propagation, and improve the fatigue life. The machined GH4169 superalloy surface hardening versus fatigue performance was studied by Wu et al. [19]. The results show that the higher the rotating bending surface microhardness is, the greater the fatigue life at room temperature is. The fatigue initiation is generally from the surface defect. Li [20] studied the effect of shot peening TC21 titanium alloy surface integrity on fatigue resistance. The results indicate that the machined hardening has an effective effect on fatigue performance. The moderate machined hardening is beneficial to the fatigue crack initiation, but can prevent the fatigue crack propagation. In addition, the excessive hardening brings about the softening layer; meanwhile, there are micro-cracks accompanied. It will also decrease the fatigue life.

In conclusions, the machined quality has an important effect on the fatigue life. The smaller residual stress and the surface roughness are, the greater the fatigue life is [21, 22]. It is necessary to improve the machined surface quality in order to prolong the fatigue life. The machined surface residual stress is mainly due to the mechanical stress bringing about the plastic deformation and the thermal stress results in the plastic strain. In the paper, the step-by-step feed cutting is put forward according to the cutting performance about the piston aluminum alloy. The forward and reverse finish cutting is also adapted to machine ZL109 aluminum-silicon piston alloy. It can bring about compressive residual stress, decrease the surface roughness, and obtain reasonable hardness.

## 2 Turning experiment

The results indicate that the modification treatment can refine grain size and improve the cutting performance and the machined aluminum-silicon alloy quality [23]. The ZL109

**Table 1** Chemical composition (wt%) of ZL109 aluminum-silicon piston alloy [24]

Si	Cu	Mg	Ni	Fe	Ti	Zn	Mn	Al
11.5–13.0	0.8–1.3	0.8–1.3	0.8–1.3	≤0.7	≤0.2	≤0.2	≤0.15	Bal

aluminum-silicon piston alloy without modification treatment is adapted to experiment. It can better reflect the effect of the step-by-step feed cutting and the forward and reverse finish cutting on improving the machined quality. Its chemical composition and physical parameters are shown in Tables 1 and 2 respectively. The sample is a cylinder, which has a dimension of  $\varnothing 120 \text{ mm} \times 15 \text{ mm}$ . The experimental material is only treated by aging treatment in nature.

The research ideas are as follows: (1) designing tool paths. The constant extrusion process is cutting, which will bring about a lot of cutting heat in process. There are elastic-plastic recovery and thermal expansion on the machined surface [26]. Obviously, the machined dimension accuracy is affected by the elastic-plastic recovery and thermal expansion. Moreover, cutting aluminum-silicon alloy can bring about the strip chip, which curls around the machined surface in process and decreases surface roughness. In addition, it will result in stress concentration and decrease fatigue life. Therefore, a reasonable tool path should be adapted to avoid the scratching by the strip chip. In the test, the step-by-step feed cutting is put forward to solve the problem. The schematic diagram for the step-by-step feed (three-step feed) is shown in Fig. 1. It can be seen from Fig. 1 that the work face will be machined in three times along the feed direction, when the step-by-step feed is used. After each feed is completed, the tool will return to the starting point and continues the next feed. (2) The forward and reverse finish cutting is to improve the machined quality through adjusting finish cutting direction. When a finish cutting is done in the direction which is opposed to a rough cutting, the residual strain of the work surface decreases so much that the surface finish of a cutting surface may be improved [27]. This is the reversal finish cutting. It was proposed by Masuko and Kumable in 1958. It is necessary to cut only proper cutting thickness. The results indicate that the proper value of the cutting depth is about 0.03–0.05 mm on carbon steel and 0.02–0.05 mm on ductile materials [27, 28].

The results indicate that the residual stress mainly depends on the thermal stress bringing about the plastic strain, when

the cutting edge is completely sharp [6, 7]. A lot of cutting heat will result in the grain enlargement in process. Then, the surface cooling and shrinkage bring about tensile residual stress eventually. The micro-structure of roughing ZL109 aluminum-silicon piston alloy surface is shown in Fig. 2. It can be seen from Fig. 2 that the grain enlargement is more than the grain refinement in rough cutting surface. The ordinary finish cutting can improve the machined quality. But it is difficult to bring about the compressive residual stress on the machined ZL109 aluminum-silicon piston alloy [29].

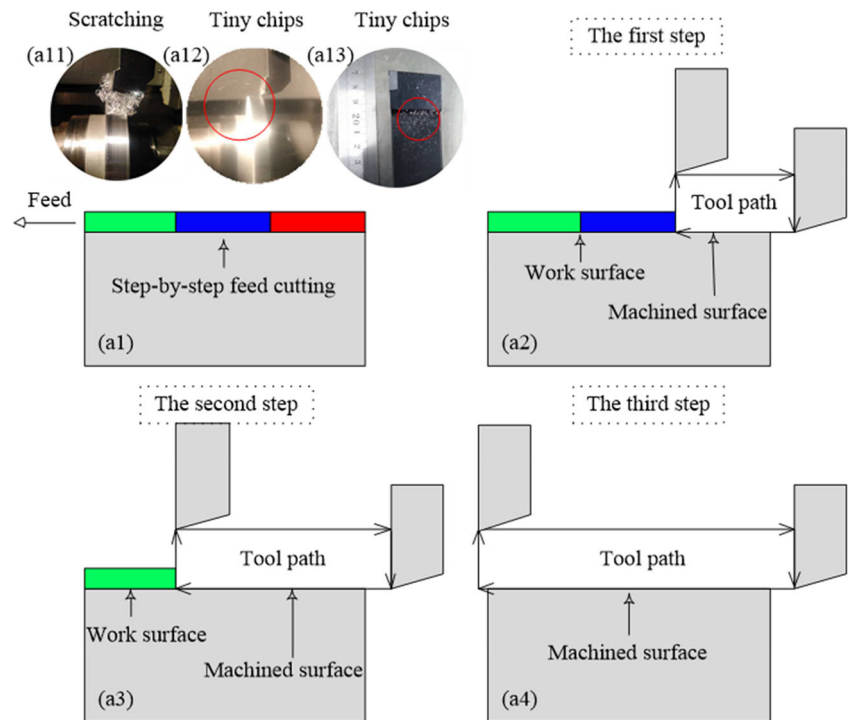
The reversal finish cutting can effectively decrease the thermal stress leading to the plastic strain. However, the results indicate that the reversal finish cutting quality depends on the cutting thickness. The high quality can be obtained when the cutting depth is very small. Therefore, the reversal finish cutting is difficult to apply in the production. The forward and reverse finish cutting is put forward to improve the machined ZL109 aluminum-silicon piston quality. After rough cutting, first finish cutting in the direction which is opposed to the rough feed cutting, then finish cutting along the roughing feed direction. This is the forward and reverse finish cutting. The high quality can be obtained when the method is adapted. The schematic diagram about forward and reverse finish cutting is shown in Fig. 3. (3) The effect of cutting parameters on the forward and reverse finish cutting quality is studied, in order to ensure the practicability. The cutting speed and feed are generally fixed in fact, but the cutting thickness is necessary to be adjusted often. However, the test studied the effect of the cutting speed, the cutting thickness, and feed on the machined quality.

The CNC (PUMA200MA) is adapted to carry out the dry turning test. The machine tool of cutting ZL109 aluminum-silicon piston alloy is shown in Fig. 4. Carbide tool is used for rough cutting (model: YD101 CCGX09T308-LC). Polycrystalline diamond insert (model: CCMW09T308F-L1, medium grain size) is adapted to finish cutting, which has a good dry cutting performance. From Fig. 4, mode of tool shank is SCLCR2525M09 (cutting direction is right) and SCLCL2525M09 (cutting direction is left) respectively. Its nose angle is 80 degree, clearance angle is 7 degree, cutting edge angle is 95 degree, shank height is 25 mm, shank width is 25 mm, tool length is 150 mm, and cutting edge length is 9.525 mm. Mode of tool in rough and finish cutting is CCGX09T308-LC (carbide) and CCMW09T308F-L1 (PCD20, medium grain size) respectively. Clearance angle is

**Table 2** Physical performance parameters of ZL109 aluminum-silicon piston alloy [25]

Tensile strength (MPa)		Expansion Coef	Shear strength (MPa)	Volume stability
Room Temp ≥200	High Temp ≥83	20–300 °C $22.03 \times 10^{-6}$	170–220	≤0.025%D

**Fig. 1** Schematic diagram for the step-by-step feed (three-step feed)



7 degree, rake angle is 0 degree, cutting edge length is 9.525 mm, and nose radius is 0.8 mm and chip free groove for the polycrystalline diamond tool.

The rough cutting parameters are fixed: the cutting speed is  $v = 150$  m/min, feed is  $f = 0.15$  mm/r, and the cutting thickness is  $a_p = 0.5$  mm. The cutting speed is  $v = 50\text{--}350$  m/min, feed is  $f = 0.05\text{--}0.30$  mm/r, and the cutting depth is  $a_p = 0.05\text{--}0.3$  mm in finish cutting. The cutting parameters are obtained by experimental research [29] and refer to the Bohai Piston Company's production experience. The experimental scheme of cutting the ZL109 aluminum-silicon piston alloy is shown in Table 3. The first group adapts the ordinary cutting. The step-by-step feed cutting is used in groups two to twenty. The finish cutting direction was in accordance with that of the rough cutting in groups one and two. The direction of the finish cutting was contrary to that of the rough cutting in group

three. The forward and reverse finish cutting is adapted in groups four to twenty.

The detailed information of making the detection sample to analyze the surface quality is shown in Fig. 5. X-ray diffraction stress analyzer (model: Xstress 3000) is adapted to measure the surface residual stress; the chromium target is used. The diffraction crystal plane is  $\langle 311 \rangle$ . Adopting the fixed angle to scan, the angle values are  $0^\circ$ ,  $15^\circ$ ,  $30^\circ$ , and  $45^\circ$  respectively. The diffraction angle is  $139.5$  degree.

The exposure time is 10 s. The surface residual stress is measured along the cutting speed and feed direction respectively. The surface residual stresses are tested 12 times for each workpiece to calculate the average value.

A portable surface roughness measuring instrument (TR200) is used to measure the machined surface roughness. The surface roughness is measured 20 times for each workpiece to calculate the average value. The micro-structure of the machined ZL109 aluminum-silicon piston alloy was measured through the three-dimensional microscopic system (Model, VHX-600E) after the detection sample is corroded. Corrosives are 20 wt% sodium hydroxide [30].

MH-6 microhardness tester is used to measure the machined surface hardness. The indenter is a diamond tetragonal body. The applied load is 25 g and the holding time is 10 s.

Its Vickers hardness ( $HV$ ) and hardening degree ( $N_H$ ) can be calculated based on the formula [31]:

$$HV = 1.8544 P/d^2 \quad (1)$$

$$N_H = (HV/HV_0) \times 100\% \quad (2)$$

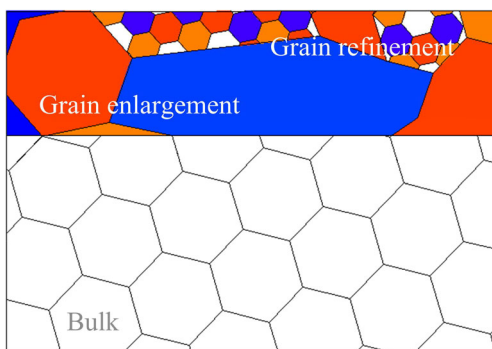
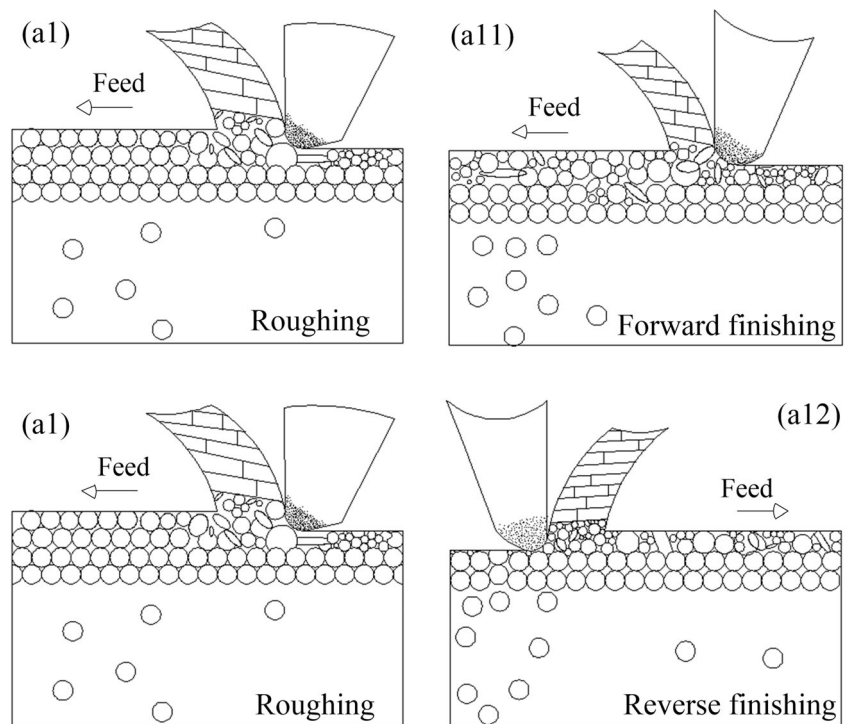


**Fig. 2** Micro-structure of roughing ZL109 aluminum-silicon piston alloy surface

**Fig. 3** Schematic diagram of forward and reverse finish cutting



where  $HV$  (MPa) embodies the machined surface hardness.  $HV_0$  (MPa) refers to the bulk hardness.  $P$  (N) represents the applied load.  $d$  (mm) is the indentation diagonal length.

### 3 Experimental results

#### 3.1 The step-by-step feed cutting

The chip morphology is the dynamic response about the machined surface with the applied load. In the process, the dynamic mechanical property of the machined surface results in the chip morphology transformation [26]. The results show that cutting the most plastic metal will generally bring about the continuous chip. The strip chips will scratch the machined

surface, increase the surface roughness, lead to the stress concentration, and decrease the fatigue life eventually [12].

There is an elastic-plastic recovery phenomenon when cutting the ZL109 aluminum-silicon piston alloy. It is difficult to control and seriously affects the machined dimension accuracy. The elastic-plastic recovery mainly depends on the mechanical and physical performances of the metal, but it is also affected by the processing [32]. We put forward the three-step feed cutting to machine the ZL109 aluminum-silicon piston alloy, to avoid the machined surface scratching by the strip chip and improve the dimension accuracy. The work surface is machined in three times along the feed direction. Machined surface topography with one-step and three-step feed cutting is shown in Fig. 6. From Fig. 6a and b, the method not only can effectively avoid chip winding and scratching but also can

**Fig. 4** Machine tool of cutting ZL109 aluminum-silicon piston alloy

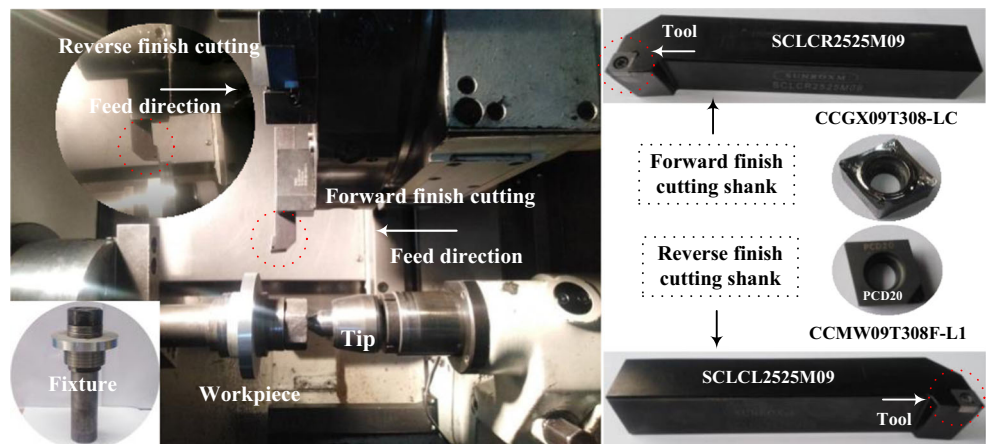


**Table 3** The experimental scheme of cutting ZL109 aluminum-silicon piston alloy

		Rough cutting		
		Cutting speed 150 m/min	Cutting depth 0.5 mm	Feed 0.15 mm/r
Finish cutting	Groups	Cutting speed (m/min)	Cutting depth (mm)	Feed (mm/r)
	1	300	0.20	0.05
	2	300	0.20	0.05
	3	300	0.20	0.05
	4	300	0.20	0.05
	5	300	0.05	0.05
	6	300	0.10	0.05
	7	300	0.15	0.05
	8	300	0.25	0.05
	9	300	0.30	0.05
	10	50	0.2	0.05
	11	100	0.2	0.05
	12	150	0.2	0.05
	13	200	0.2	0.05
	14	250	0.2	0.05
	15	350	0.2	0.05
	16	300	0.2	0.10
	17	300	0.2	0.15
	18	300	0.2	0.20
	19	300	0.2	0.25
	20	300	0.2	0.30

cut the elastic-plastic recovery and the thermal expansion with minimum cutting thickness. Moreover, the cutting force and heat is minimum because the cutting depth is very small, so much that there is smaller elastic-plastic recovery and thermal expansion on the machined surface. From Fig. 6 a1 and b1, the deformation marks of the one-step feed cutting surface (the ordinary cutting) are more obvious than those of the three-step feed cutting surface.

In addition, the three-step feed cutting can provide a good heat dissipation environment under the dry cutting condition. It should reduce the tool temperature in process and decrease the tool wear [33]. Meanwhile, the method can decrease the effect of the thermal stress bringing about the plastic strain on the residual stress. Therefore, it can effectively decrease the residual stress, and even lead to the compressive residual stress.

The results of Huang et al. [34] indicate that the fatigue life mainly depends on the maximum tensile residual stress. The smaller the real residual stress  $\sigma_{\text{real}}$  is, the higher the fatigue life is. The real stress  $\sigma_{\text{real}}$  is as follows:

$$\sigma_{\text{real}} = \sigma_{\text{load}} + \varphi_{\text{rs}} + \varphi_{\text{scrs}} \quad (3)$$

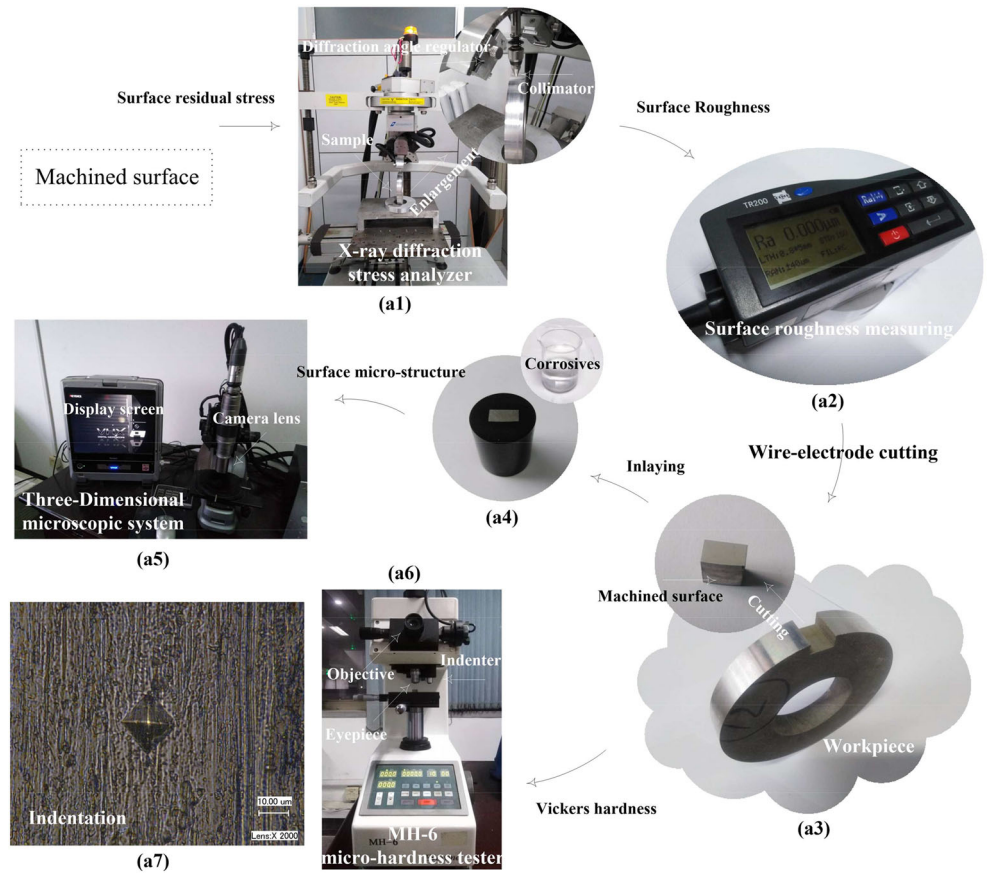
where  $\sigma_{\text{load}}$  embodies the tensile residual stress is applied.  $\varphi_{\text{rs}}$  refers to the machining bringing about the

residual stress.  $\varphi_{\text{scrs}}$  represents excrescent stress because the surface topography leads to the stress concentration. Therefore, the compressive residual stress on the machined surface can improve the fatigue life effectively. Of course, the tensile residual stress will decrease the fatigue life obviously.

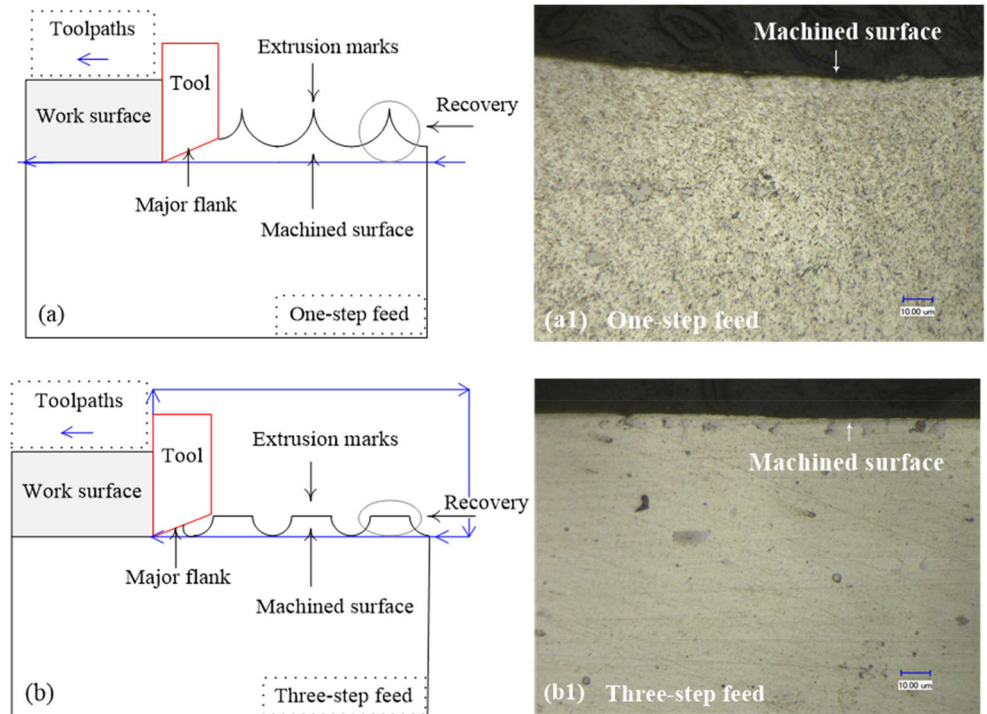
Comparison between one-step and three-step feed processing quality is shown in Fig. 7. It can be seen from Fig. 7 that the one-step and three-step feed cutting results in surface roughness of about 0.4  $\mu\text{m}$ . But the fluctuation of the three-step feed method brings about the surface roughness being slight than that of the one-step feed cutting. Under the same cutting condition, the one-step feed turning leads to the tensile residual stress, but the three-step feed turning can bring about the compressive residual stress. Moreover, the fluctuation range of the residual stress is very small, if the three-step feed cutting is adapted. It can improve the fatigue life. The three-step feed cutting surface hardness is higher than ordinary cutting.

In addition, there are a few of the pitting corrosion on the machined surface. Obviously, it can improve the piston wear resistance. Therefore, the three-step feed cutting can not only avoid the chip scratching the machined surface effectively but also improve the dimension accuracy, processing quality, and fatigue life. Therefore, the three-step feed cutting is also adapted to the rough cutting in the next test.

**Fig. 5** Detailed information of making the detection sample to analyze the machined surface quality



**Fig. 6** Machined surface topography with one-step and three-step feed cutting



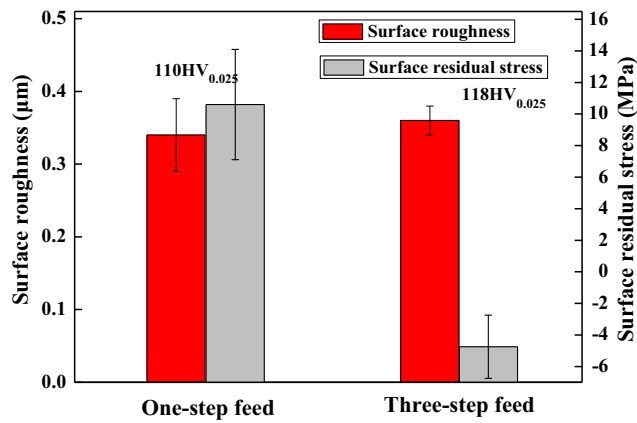


Fig. 7 Comparison between one-step and three-step feed processing quality

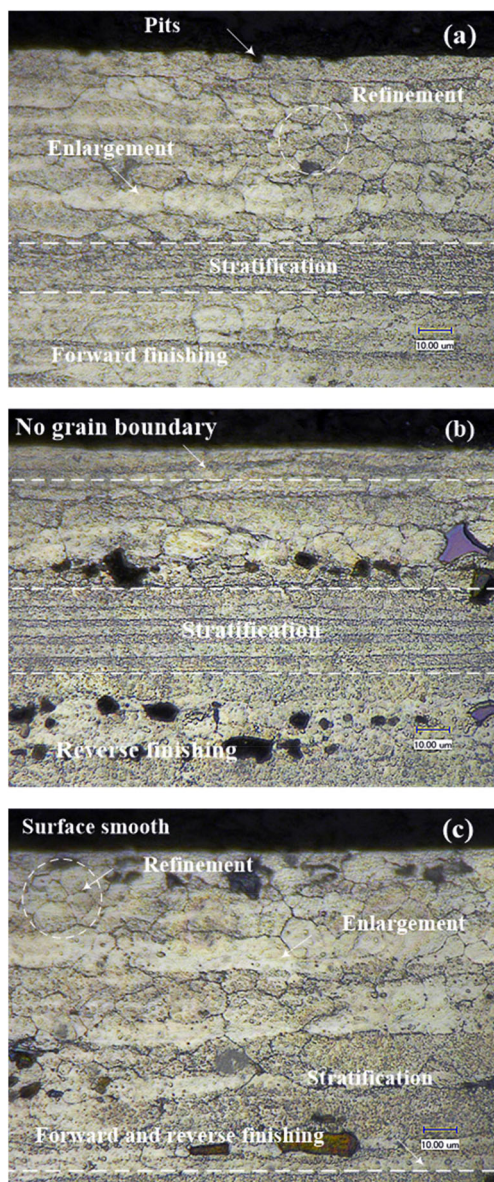


Fig. 8 Machined surface micro-structure with forward, reverse, and forward and reverse finish cutting

### 3.2 Forward and reverse finish cutting method

The reversal finish cutting method was put forward by Masuko and Kumabe [27] in 1958. It can effectively remove the crystals in the flow direction of the rough cutting surface, meanwhile bringing about a shallow metamorphic layer. In addition, the reverse finish cutting can result in the high wear resistance surface without residual strain and very small surface roughness. But the results indicate that the high quality is obtained through the reverse finish cutting only when the cutting thickness is 0.03–0.05 mm. The effect of the reversal finish cutting on residual stress is not studied. Based on the results, Yang et al. [28] studied the effect of the reverse finish cutting on the residual stress of copper and steel 45.

The results show that the reverse finish cutting is suitable for the medium-soft and tough metals. But the high machined quality is only obtained when the cutting depth is 0.02–0.05 mm. There are different conclusions about the machined surface hardness. The result of Yang et al. indicates that the reverse finish cutting surface hardness is improved significantly.

In conclusion, the reversal finish cutting quality depends on the small cutting depth. Therefore, it has a poor engineering practicability. The forward and reverse finish cutting is put forward to machine the ZL109 aluminum-silicon piston alloy in the test.

Machined surface micro-structure with forward, reverse, and forward and reverse finish cutting is shown in Fig. 8. From Fig. 8a, there exists a serious grain damage phenomenon in the forward finish cutting surface. In addition, there are grain damage, grain refinement, and enlargement phenomena in the sub-surface. The grain distribution shows a certain orientation. It can be seen from Fig. 8b that there is no grain boundary in the machined surface after the reverse finish cutting. The thickness is about 15 μm. Moreover, there is the shrinkage phenomenon in the micro-structure of the ZL109 aluminum-silicon piston alloy, which is formed in casting. It

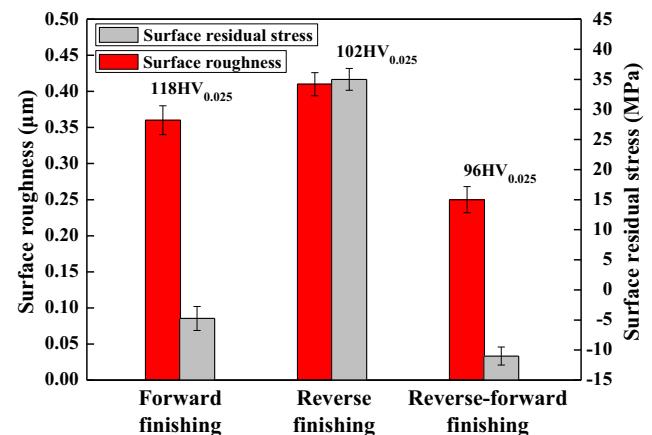


Fig. 9 Comparison of the forward, reverse, and forward-reverse finish cutting quality



will seriously decrease the mechanical performance and fatigue life.

In Fig. 8c, there is no grain boundary in the machined surface about 5 μm, when the forward and reverse finish cutting is adapted in the experiment. The grain refinement is obvious in the sub-surface. There also exist grain growth and elongation phenomena in the sub-surface. The grain distribution orientation is poor. In addition, there is an obvious stratification phenomenon in the micro-structure of the ZL109 aluminum-silicon piston alloy. It is mainly due to the fluctuation of the liquid rate during the cast. The forward and reverse finish cutting surface is smoother than that of the reverse finish cutting surface. Moreover, the grain refinement phenomenon in then sub-surface is also obvious. There is generally no grain growth and elongation phenomenon. It shows that the thermal stress brings about the tensile residual stress being very small,

so it is prone to result in the compressive residual stress and improve the fatigue life.

Arola and Williams [12] put forward the greater the stress concentration of the machined surface is, the lower the fatigue life is. Neuber [35] comes up with the machined surface morphology having a characteristic that the distribution of the adjacent notches is continuous. The stress concentration coefficient of the machined surface is as follows:

$$K_t = 1 + n \sqrt{\lambda \frac{R_Z}{\rho}} \tag{4}$$

where λ represents the ratio of the micro-groove interval to depth. It is difficult to measure and λ = 1 generally. ρ refers to the mean bottom radius of the micro-groove. n embodies the

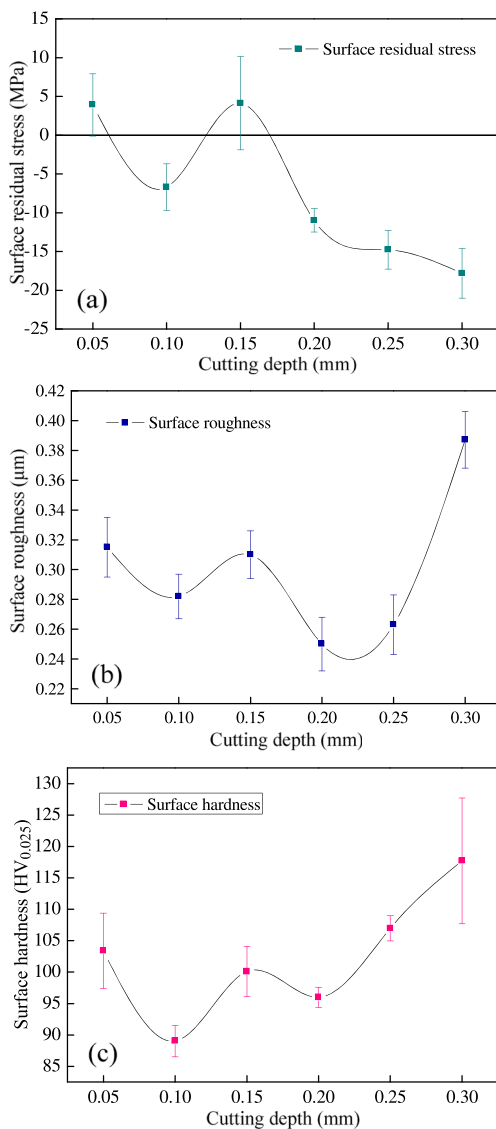


Fig. 10 Processed quality versus the cutting depth under forward and reverse finish cutting

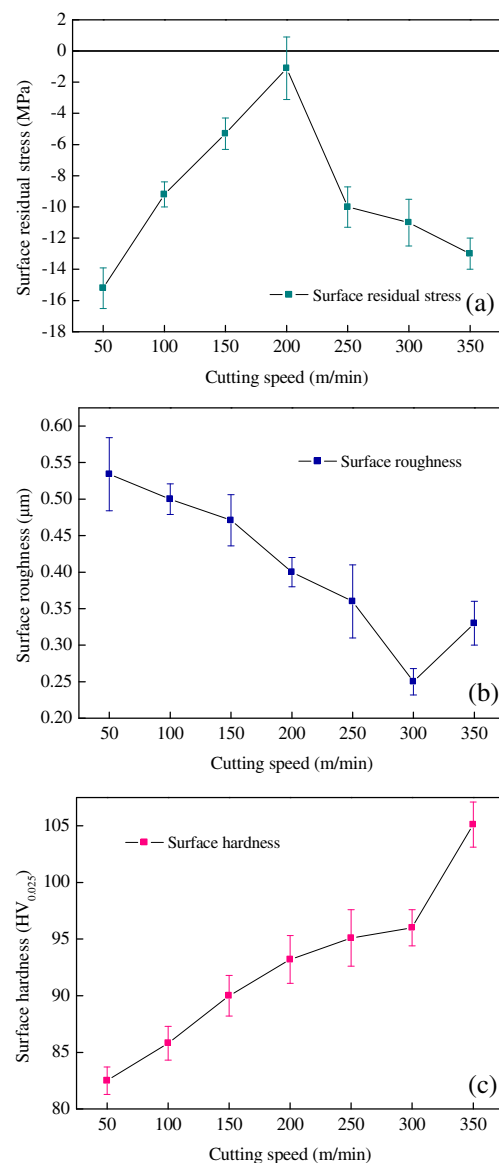


Fig. 11 Machined quality versus the cutting speed under forward and reverse finish cutting

stress state ( $n = 1$  for shear stress;  $n = 2$  for tensile stress). “GB 1031-83” (it is equivalent to ISO 468-83) is used to transform the surface roughness  $R_a$  into  $R_z$  equivalently. It can be seen from Eq. (4) that the bigger the machined surface roughness  $R_z$  is, the greater the surface stress concentration coefficient, and then the lower the fatigue life.

The comparison of the forward, reverse, and forward-reverse finish cutting quality is shown in Fig. 9. It can be seen from Fig. 9 that under the cutting thickness  $a_p = 0.20$  mm, the reverse finish cutting quality is bad than that of the forward finish cutting. But the forward and reverse finish cutting brings about the high quality than the forward finish cutting. When the cutting speed is 300 m/min, the cutting depth is 0.20 mm, and feed is 0.05 mm/r, the forward and reverse finish cutting results in the compressive surface stress of about  $-11$  MPa, the surface roughness is  $0.25 \mu\text{m}$ , and surface hardness is  $96 \text{HV}_{0.025}$ .

### 3.3 Machined quality versus the cutting parameters with forward and reverse finish cutting

#### 3.3.1 The effect of the cutting thickness on the machined quality

It can be seen from Section 3.2 that the forward and reverse finish cutting method can improve the machined quality. In production, the cutting speed and the feed are fixed generally. The cutting depth has to be adjusted in order to obtain the dimension. Therefore, it is inevitable to study the effect of the cutting thickness on the machined quality.

Processed quality versus cutting depth under forward and reverse finish cutting is shown in Fig. 10. In Fig. 10a, when the forward and reverse finish cutting method is adapted, the surface residual stress is very small under the different cutting thicknesses. The forward and reverse finish cutting brings about the tensile residual stress only when the cutting depth is 0.05 mm and 0.15 mm. Moreover, the tensile residual stress is less than 5 MPa. It can lead to the compressive residual stress when the cutting depth is 0.10 mm, 0.20 mm, 0.25 mm, and 0.30 mm. And the compressive residual stress decreases with the cutting depth increasing, when the cutting thickness is more than 0.20 mm. It is mainly due to the forward and reverse finish cutting method effectively decreasing the thermal stress components in residual stress. In addition, the fluctuation of the residual stress is the smallest, if the cutting depth is  $a_p = 0.20$  mm.

It can be seen from Fig. 10b that the forward and reverse finish cutting brings about the surface roughness of less than  $0.40 \mu\text{m}$  at different cutting depths. The surface roughness increases sharply when the cutting thickness is 0.30 mm.

From Fig. 10c, the forward and reverse finish cutting result in the surface hardness is about  $90\text{HV}_{0.025}$ – $120 \text{HV}_{0.025}$  at different cutting depths. The surface hardness increases

rapidly when the cutting depth increases to 0.3 mm; meanwhile, the fluctuation of the hardness is obvious. In addition, the fluctuation of the machined surface hardness is very small when the cutting depths are  $a_p = 0.20$  mm and  $a_p = 0.25$  mm.

There is the same trend between the surface hardness, surface roughness, and residual stress versus the cutting depth increases, when the cutting depth is 0.05–0.20 mm. Increasing the cutting depth can result in the cutting temperature to increase. Meanwhile, the proportion of the thermal stress bringing about the residual stress will further increase. The cutting is prone to result in the tensile residual stress. But the forward and reverse finish cutting can effectively decrease the surface residual stress. Therefore, the compressive residual stress decreases even when the cutting depth is increasing.

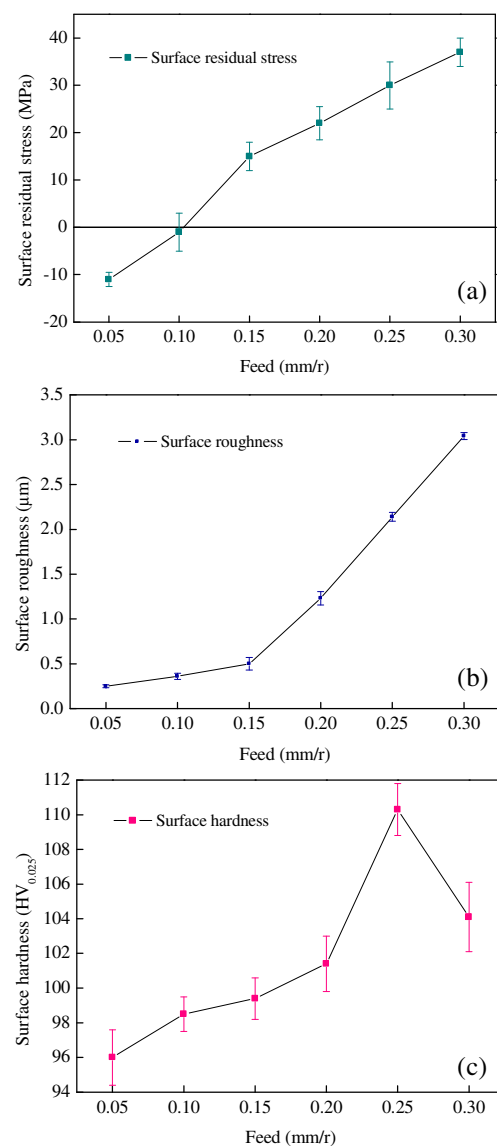


**Fig. 12** Processed quality versus the feed under forward and reverse finish cutting

**Table 4** Advantages and disadvantages of the machined surface strengthening technology

Barreling [42]	Principle	Machined surface is rolled to bring about plastic deformation, to fill the depression with the protrusion and improve machined quality.
	Advantages	<ul style="list-style-type: none"> <li>① Increasing the surface hardness.</li> <li>② Decreasing surface roughness.</li> <li>③ Bring about the compressive residual stress.</li> </ul>
	Disadvantages	<ul style="list-style-type: none"> <li>① Barreling quality depends on machined quality.</li> <li>② Requiring special equipment.</li> <li>③ Increasing the production cost.</li> </ul>
Shot peening [43]	Principle	The projectile impacts the machined surface to bring about the plastic deformation and improve the machined quality.
	Advantages	<ul style="list-style-type: none"> <li>① Increase the surface hardness.</li> <li>② Bring about the compressive residual stress.</li> <li>③ Strengthening thin-walled and complex parts.</li> </ul>
	Disadvantages	<ul style="list-style-type: none"> <li>① Deteriorating the surface roughness.</li> <li>② The surface hardening degree is not easy to control.</li> <li>③ Increasing production cost.</li> </ul>
Pre-stressed processing [44]	Principle	The parts are pulled in process. The shrinkage of the internal material results in the compressive residual stress after tensile stress is released.
	Advantages	<ul style="list-style-type: none"> <li>① Improving the machined quality in process.</li> <li>② Improving production efficiency.</li> <li>③ Bring about the compressive residual stress.</li> </ul>
	Disadvantages	<ul style="list-style-type: none"> <li>① The pre-stressed application should be considered in part design.</li> <li>② Requiring special equipment.</li> <li>③ Increasing production cost.</li> </ul>
Reversal finish cutting [27]	Principle	The finish cutting direction is opposite to that of the rough cutting.
	Advantages	<ul style="list-style-type: none"> <li>① Improving the machined quality in process.</li> <li>② No special equipment is required;</li> <li>③ Decreasing the production cost.</li> </ul>
	Disadvantages	<ul style="list-style-type: none"> <li>① The cutting thickness is too small to be applied.</li> <li>② Lacking of applied research extensively.</li> </ul>

### 3.3.2 The effect of the cutting speed on the machined quality

The machined quality versus the cutting speed under forward and reverse finish cutting is shown in Fig. 11. It can be seen from Fig. 11a that the forward and reverse finish cutting ZL109 aluminum-silicon piston alloy can bring about the compressive residual stress, when the cutting speed is 50–350 m/min. It shows that the method can decrease the residual stress due to the thermal stress, and dominate the characteristic of the surface residual stress. The surface residual stress gradually increases when the cutting speed is 50–200 m/min. It is due to that the cutting temperature is relatively low when the cutting speed is small, so that the production and characteristic of the residual stress mainly depend on mechanical stress [36–38].

The results show that the proportion of heat generation on the shear plane flowing into the chips increases. So that the higher the cutting speed is, the more heat is taken away by the chips, and the lower the cutting temperature is [39]. And the thermal stress bringing about the tensile residual stress will relatively decrease and the surface residual stress gradually decreases when the cutting speed is 200–350 m/min.

The proportion of heat generation on the shear plane flowing into the chips is as follows [39]:

$$R_1 = \frac{1}{1 + 1.33 \sqrt{\frac{a_1 \varepsilon}{v a_c}}} \tag{5}$$

- $a_1 = \frac{\lambda_1}{c_1 \rho_1}$  coefficient of temperature conductivity
- $\lambda_1$  coefficient of thermal conductivity
- $c_1$  specific heat capacity of the chips
- $\rho_1$  chip density
- $\varepsilon$  shear strain
- $a_c$  cutting thickness
- $v$  cutting speed

It can be seen from the above formula that  $R_1$  will increase with the cutting speed and thickness increasing. But the fluctuation of the cutting speed is larger than that of the cutting thickness. So that the influence of the cutting speed on  $R_1$  is more greater than that of the cutting thickness.

It can be seen from Fig. 11b that the surface roughness decreases gradually when the cutting speed is 50–300 m/min. Cutting aluminum alloy is prone to bring about the built-up

edge and burr when the cutting speed is low, so that the surface roughness is large [29, 40]. But when the cutting speed is 350 m/min, the surface roughness is larger than that of the cutting speed 300 m/min. The results indicate that the high spindle speed will lead to tool vibration and deteriorate process condition, and further result in the surface roughness increases [39–41]. From Fig. 11c, the machined surface hardness gradually increases with the cutting speed increasing. The machined surface hardness is 105.1HV0.025 when the cutting speed is 350 m/min, in which hardening degree is about 131%.

### 3.3.3 The effect of the feed on the machined quality

The machined quality versus the feed under forward and reverse finish cutting is shown in Fig. 12. As can be seen from Fig. 12a, the surface residual stress increases obviously with the feed increasing. The larger the feed is, the more the cutting heat and the larger the surface residual stress is [6, 7, 41]. The compressive residual stress can be obtained when the feed is 0.05–0.10 mm/r. But the forward and reverse finish cutting will bring about the tensile residual stress when the feed is 0.15–0.30 mm/r.

From Fig. 12b, the surface roughness increases rapidly with the feed increasing. The surface roughness is less than 0.5  $\mu\text{m}$  when the feed is 0.05–0.15 mm/r. The surface roughness is more than 1.0  $\mu\text{m}$  when the feed is 0.20–0.30 mm/r. Therefore, the small feed is beneficial to obtain the high machined quality.

It can be seen from Fig. 12c that when the feed is 0.05–0.25 mm/r, the larger the feed is, the larger the machined surface hardness is. But the surface hardness decreases when the feed is 0.30 mm/r. It is mainly due to the surface shear stress more than the limit [17]. The over-hardening will result in the spalling and crack, then decrease the fatigue life.

## 4 Discussion

At present, the surface strengthening technology has the rolling, the shot peening, and the pre-stressed machining, etc. [42–44]. The rolling and the shot peening are used to strengthen the machined surface and improve the fatigue life, which belongs to post-processing. The pre-stressed machining can improve the machined quality in the process and decrease the production cost.

In addition, the reversal finish cutting is put forward by Masuko and Kumabe [27]. It can also improve the machined quality in process. Then, Yang et al. [28] studied the effect of the reverse finish cutting on the machined surface residual stress. The results indicate that the reverse finish cutting can only bring about the high machined quality when the cutting depth is 0.02–0.05 mm.

The results indicate that the forward and reverse finish cutting can improve the machined quality of ZL109 aluminum-silicon piston alloy in the process. The range of the cutting

parameters is suitable for the turning. It can be used to guide the production. The advantages and disadvantages of the machined surface strengthening technology are shown in Table 4.

## 5 Conclusion

In the paper, the step-by-step feed cutting and the forward and reverse finish cutting are put forward. The machined quality of the ordinary cutting, the step-by-step finish cutting, the reverse finish cutting, and the forward and reverse finish cutting are studied. The conclusions are as follows:

- (1) The step-by-step feed cutting not only can effectively avoid chip winding and scratching but also can cut the elastic-plastic recovery and the thermal expansion with minimum cutting thickness. Moreover, the cutting force and heat is minimum because the cutting depth is very small, so much that there is small elastic-plastic recovery and thermal expansion on the machined surface.
- (2) The step-by-step feed cutting can provide a good heat dissipation environment under the dry cutting condition, decreasing the tool temperature in process.
- (3) The forward and reverse cutting can bring about the high machined quality in reasonable cutting parameters. The machined quality of the forward and reverse finish cutting is more greater than that of the ordinary cutting.
- (4) The forward and reverse finish cutting can effectively decrease the thermal stress bringing about the tensile residual stress. The characteristic of the surface residual stress depends on the mechanical stress results in the compressive residual stress. So the larger the cutting thickness is, the smaller surface residual stress is, when the cutting depth is 0.15–0.30 mm in the forward and reverse finish cutting.

**Funding information** This work was supported by the National Natural Science Foundation of China (51605260), the Key Research and Development Program of Shandong Province - Public Welfare Special (2017GGX30144, 2018GGX103043), and the Young Scholars Program of Shandong University (2018WLJH57).

## References

1. Wang JF, Xie JP, Liu ZX, Li JW, Weng YG, Wang MX (2005) Review on the research and application of Al-Si piston alloy at home and abroad. *Foundry* 54(1):24–27
2. Konečná R, Nicoletto G, Kunz L, Svoboda M, Bača A (2014) Fatigue strength degradation of AlSi12CuNiMg alloy due to high temperature exposure: a structural investigation. *Procedia Eng* 74: 43–46
3. Joyce MR, Styles CM, Reed PAS (2003) Elevated temperature short crack fatigue behaviour in near eutectic Al–Si alloys. *Int J Fatigue* 25(9):863–869

4. Zeren M (2007) The effect of heat-treatment on aluminum-based piston alloys. *Mater Des* 28:2511–2517
5. El-Axir MH (2002) A method of modeling residual stress distribution in turning for different materials. *Int J Mach Tool Manu* 42(9): 1055–1063
6. Papahn H, Bahemmat P, Valipour A (2014) Ultrasonic measurements of residual stresses caused by severe thermomechanical deformation during FSW. *Exp Mech* 54(9):1587–1596
7. Wang SY, Ai X, Zhao J, Li ZL, Meng H (2005) Effect of cutting speed on residual stress of workpiece by using FEM. *Tool Eng* 39(9):33–36
8. El-Helieby SOA, Rowe GW (1980) A quantitative comparison between residual stresses and fatigue properties of surface-ground bearing steel (En 31). *Wear* 58(1):155–172
9. Jeelani S, Musial M (1986) Dependence of fatigue life on the surface integrity in the machining of 2024-T351 aluminium alloy — unlubricated conditions. *J Mater Sci* 21(1):155–160
10. James MN, Hughes DJ, Chen Z, Lombard H, Hattingh DG, Asquith D, Yates JR, Webster PJ (2007) Residual stresses and fatigue performance. *Eng Fail Anal* 14(2):384–395
11. Zou X, Liang YL, Wu ZL, Qin SJ, Hu JJ (2017) Effects of abrasive waterjet peening on surface integrity and fatigue properties of carburizing GDL-1 steel. *China Surf Eng* (2):47-53
12. Arola D, Williams CL (2002) Estimating the fatigue stress concentration factor of machined surfaces. *Int J Fatigue* 24(9):923–930
13. Novovic D, Dewes RC, Aspinwall DK, Voice W, Bowen P (2004) The effect of machined topography and integrity on fatigue life. *Int J Mach Tool Manu* 44(2–3):125–134
14. Ardi DT, Li YG, Chan KHK, Blunt L, Bache MR (2014) The effects of machined topography on fatigue life of a nickel based superalloy. *Procedia CIRP* 13:19–24
15. Andrews S, Sehitoglu H (2015) A computer model for fatigue crack growth from rough surfaces. *Int J Fatigue* 22(7):619–630
16. Suraratchai M, Limido J, Chieragatti R (2008) Modelling the influence of machined surface roughness on the fatigue life of aluminium alloy. *Int J Fatigue* 30(12):2119–2126
17. Xu XC, Liu DX, Zhang XH, Liu CS, Liu D, Zhang WC (2019) Influence of ultrasonic rolling on surface integrity and corrosion fatigue behavior of 7B50-T7751 aluminum alloy. *Int J Fatigue* 125:237–248
18. Li XH, Li WH, Wang CW, Yang SQ, Shi HT (2018) Surface integrity and anti-fatigue performance of TC4 titanium alloy by mass finishing. *China Surf Eng* 31(1):15–25
19. Wu DX, Zhang DH, Yao CF (2017) Effect of surface integrity of turned GH4169 superalloy on fatigue performance. *J Aeronaut Mater* 37(6):59-67
20. Li SP, Liu DX, Li RH, Xia ML, Zhang W, Mj Q, Du DX (2012) Influence of shot peening and surface integrity on fatigue properties of TC21 titanium alloy. *Mech Sci Technol Aerospace Eng* 31(12): 1418–1423
21. Javidi A, Rieger U, Eichlseder W (2008) The effect of machining on the surface integrity and fatigue life. *Int J Fatigue* 30(10–11): 2050–2055
22. Yao CF, Tan L, Ren JX, Lin Q, Liang YS (2014) Surface integrity and fatigue behavior for high-speed milling Ti–10V–2Fe–3Al titanium alloy. *J Fail Anal Prev* 14(1):102-112
23. Prema S, Shreeshaail GY, Chandrashekharaiiah TM (2015) Analysis of machining parameter and surface finish of Al-Si alloys with grain refiners and/or modifier. *Mater Sci Forum* 830-831:91–94
24. Sun H, Li A, Zhou Y, Liao XL, Ge DJ (2019) Dry wear characteristics of machined ZL109 aluminum-silicon alloy surface under unidirectional and reciprocating rolling-contact friction. *Surf Topogr Metrol Prop* 8(1): 015001
25. Shao F, Liu ZQ, Wan Y, Zhang BG (2010) Diffusion wear for PCD tools cutting aluminum alloy ZL109 based on thermodynamics. *J Tianjin Univ* 43(4):315-321
26. Wang B, Liu ZQ (2016) Effect of material dynamic properties on the chip formation mechanism during high speed machining. *Scientia Sinica Technol* 46(1):1–19
27. Masuko M, Kumabe J (1959) A few new methods of metal cutting to get a fine surface at low speed: sub-zero-, reversal finish-, and ultrasonic cutting. *Bulletin JSME* 2(7):487–494
28. Yang NX, Qi XY, Chen BJ, Xu H (1991) A study of adjusting residual stresses in machined surface by reversal finish cutting. *J South China Univ Technol (Nat Sci Ed)* 19(2):15-21
29. Sun H, Li AH, Zhou YH, Hou GM (2019) Study of surface quality in turning of aluminum-silicon alloy ZL109. *Tool Engineering* 53(04):8–13
30. Lin C, Wu SS, Lü SL, An P, Wan L (2013) Effects of ultrasonic vibration and manganese on microstructure and mechanical properties of hypereutectic Al–Si alloys with 2%Fe. *Intermetallics* 32: 176–183
31. Fu XL (2007) Constitutive equation for 7050 aluminum alloy at high temperatures. M.S. Dissertation, Shandong University, China
32. Hill SI, Kuhlman SH, Wang K, Belwafa J, Chen X (2009) Bake-hardening effect of dual phase steels. SAE Technical Paper 2009-01-0796
33. Li AH, Zhao J, Luo HB, Pei ZQ, Wang ZM (2012) Progressive tool failure in high-speed dry milling of Ti-6Al-4V alloy with coated carbide tools. *Int J Adv Manuf Technol* 58(5–8):465–478
34. Huang W, Zhao J, Ai X, Wang GJ, Tao HW (2018) Influence of tool path strategies on fatigue performance of high-speed ball-end-milled AISI H13 steel. *Int J Adv Manuf Technol* 94(1–4):371–380
35. Neuber H (1958) Theory of notch stress, vol 204. Springer-Verlag, Berlin
36. Wang ZQ, Liu CF (2015) Literature review of residual stress on the surface in the cutting. *Aeronaut Manuf Technol* 06:28–32
37. Niu JT, Liu ZQ, Ai X, Wang GJ, Duan R (2019) Characteristics of machined surface integrity in face milling Al-Li alloy 2A97 with carbide inserts. *Int J Adv Manuf Technol* 101(1–4):839–848
38. Wang GJ, Liu ZQ, Ai X, Huang WM, Niu JT (2018) Effect of cutting parameters on strain hardening of nickel–titanium shape memory alloy. *Smart Mater Struct* 27(7):075027
39. Ai X (2003) High speed machining technology. National Defense Industry Press, Beijing
40. Xing DL, Zhang JH, Shen XH, Zhao YF (2011) Experimental study on surface roughness of aluminum alloy in micro-milling process. *Manuf Technol Mach Tool* 03:36–39
41. Zhou YH, Sun H, Li AH, Lv MH, Xue CY, Zhao J (2019) FEM simulation-based cutting parameters optimization in machining aluminum-silicon piston alloy ZL109 with PCD tool. *J Mech Sci Technol* 33:3457–3465
42. Kuznetsov VP, Dmitriev AI, Anisimova GS, Semenova YV (2016) Optimization of nanostructuring burnishing technological parameters by Taguchi method. *IOP Conf Ser Mater Sci Eng* 124(1): 012022
43. Damon J, Dietrich S, Vollert F, Gibmeier J, Schulze V (2018) Process dependent porosity and the influence of shot peening on porosity morphology regarding selective laser melted AISi10Mg parts. *Addit Manuf* 20:77–89
44. Zhou Z, Guo D (1987) Pre-stressed machining. *Proceedings of the 9th ICPR* 1: 257-263